Normal Rack Grid Generation Method for Screw Machines with Large Helix Angles

IOP Conf. Series: Materials Science and Engineering **604** (2019) 012011 doi:10.1088/1757-899X/604/1/012011

Normal Rack Grid Generation Method for Screw Machines with Large Helix Angles

Yang Lu, Ahmed Kovacevic and Matthew Read

City, University of London, Centre for Compressor Technology, London, UK
Email: yang.lu.4@city.ac.uk

Abstract. Improving the efficiency of the screw machine is highly significant for industry. Numerical simulation is an important tool in developing these machines. The 3D computational fluid dynamic simulation can give a valuable insight into the flow parameters of screw machines. However, it is currently difficult to generate high quality computational grids required for screw rotors with large helix angle. This is mainly due to the excessively high cell skewness of the rotors with large helix angel, which would introduce errors in numerical simulation. This paper presents a novel grid generation algorithm used for the screw rotors with large helix angel. This method is based on the principles developed for the grid generation in transverse cross-section. Such mesh is generated by SCORG^{TM} using normal rack grid generation method which means numerical meshes are generated in a plane normal to the pitch helix line. The mesh lines are then parallel to the helix line and thus an orthogonal mesh will be produced. The main flow and leakage flow directions are orthogonal to the mesh, potentially reducing numerical diffusion. This developed algorithm could also be employed for single screw machines.

1. Introduction

Rotary screw machines are positive displacement machines. The operating principle of screw machines has been known for over 100 years. The main rotor meshes with the gate rotor in a fix casing together forming different working chambers which volume depends on the rotation angle, as shown in Figure 1. The working process can be divided into suction, compression and discharge.

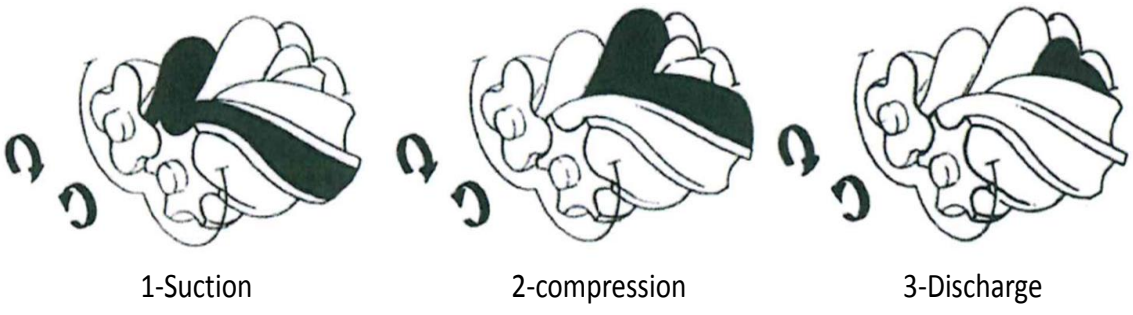

Figure 1 Operating stages in a twin-screw compressor[1].

Screw machines have been studied for decades from rotor profiles design to numerical analysis using lumped parameter models and 3-D CFD simulation to experimental investigates. However, the 3-D numerical simulation of screw machines is highly difficult because of the complex rotor geometry and

the volume-changing chambers with very small clearances between the rotors and casing. The finite volume method (FVM) commonly employed in CFD codes which allows fast and accurate solution of the governing equations for fluid flow within complex geometries. The calculated results of algebraic equations are more conservative than other discretization methods like FDM or FEM [2]. To use this method, the working chamber between the rotors and casing must be represented by discretized volumes constructed with mesh points. Kovacevic [3] has developed a computer program SCORG (Screw Compressor Rotor Grid Generator), which uses an algebraic grid generation method together with boundary adaptation, transfinite interpolation, grid orthogonalisation and smooth to generate hexahedral numerical mesh for twin screw machines. The analytical rack was firstly used for decomposition of the rotor in the transverse cross section to split the rotor domain to two O blocks as shown in Figure 2. The two O blocks together form a composite grid. Kovacevic [4] has successfully predicted the flow state, heat transfer and fluid-structure interaction using the mesh generated by SCORG. Voorde et al [5] constructed a block structured mesh using the gradient lines and the potential lines to split the fluid domain in the transverse planes. Rane [6] proposed the algebraic grid generation method which combined the advantages of algebraic and differential method together. In this method, the boundary nodes are firstly distributed on the transverse rack and casing circle and these nodes remain steady with respect to the rotor. Recently, Rane [7-9] proposed new developments of SCORG on the grid generation for variable geometry rotors, accurate representation of clearances and multiphase screw machines.

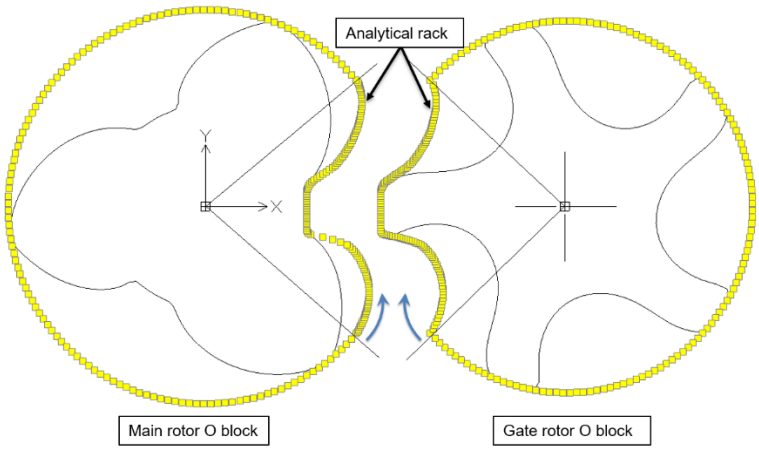

Figure 2 Analytical rack as the splitting line.

Vierendeels [1] compared two different velocity flow through a square discretised with structured grid. As shown in Figure 3, when the flow direction is not aligned to the grid direction, the interface between two flows is not distinctive. When the flow direction is changed to orthogonal to the grid direction, then less numerical diffusion produced by mesh alignment.

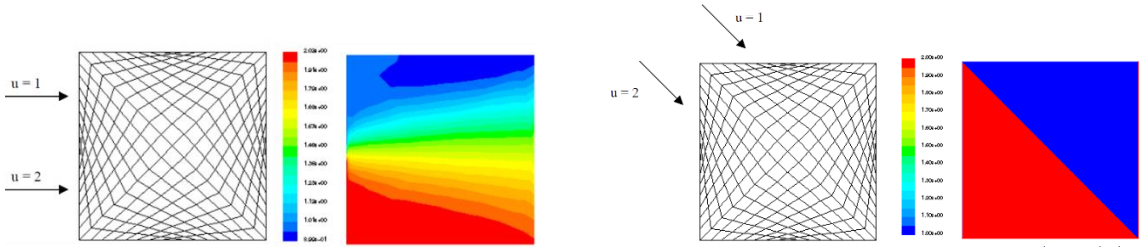

(a) Not aligned mesh (b) Aligned mesh

Figure 3 Comparison of the flow direction

So far the meshes of the fluid domain are generated in the transverse planes which cut both the rotors perpendicular to the rotor axes. The main flow and leakage flow directions are most likely along the helix line. The flow direction cannot generally be aligned with a grid generated in the transverse plane. Comparing to transverse mesh generation, a different method using the normal rack to split the fluid domain is proposed in this paper. It is more convenient if the main rotor and gate domains are cut by their normal plane respectively, so the grids can be generated in the normal plane. For vacuum pumps and oil-free compressors the leakage loss is significant, and the helix angle is relatively large to increase the sealing points. The 3-D cell skewness can therefore become large for this kind of machines, which will introduces errors in numerical simulation.

2. Coordinate system

To start the grid generation procedure in the normal plane, the right-handed Cartesian coordinate systems are specified firstly for the positions and orientations of the physical domain of two meshing rotors. The global coordinate system is $S(X,Y,Z)$. All the other coordinate systems are defined in the global coordinate system. Two rotor coordinate systems $S_1(X_1,Y_1,Z_1)$ and $S_2(X_2,Y_2,Z_2)$ are defined to generate fix main and gate rotor profiles separately. The rotor transform local coordinate systems $S_{01}(X_{01},Y_{01},Z_{01})$ and $S_{02}(X_{02},Y_{02},Z_{02})$ are defined to generate main and gate rotor profiles in different transverse cross sections along the Z-axis separately. The rotor normal local coordinate systems $S_{11}(X_{11},Y_{11},Z_{11})$ and $S_{12}(X_{12},Y_{12},Z_{12})$ are defined to generate main and gate rotor profiles and rack in different normal cross sections to the pitch helix line. One normal rack coordinate system $S_{13}(X_{13},Y_{13},Z_{13})$ is defined to transform the rack to the rotor normal local coordinate system.

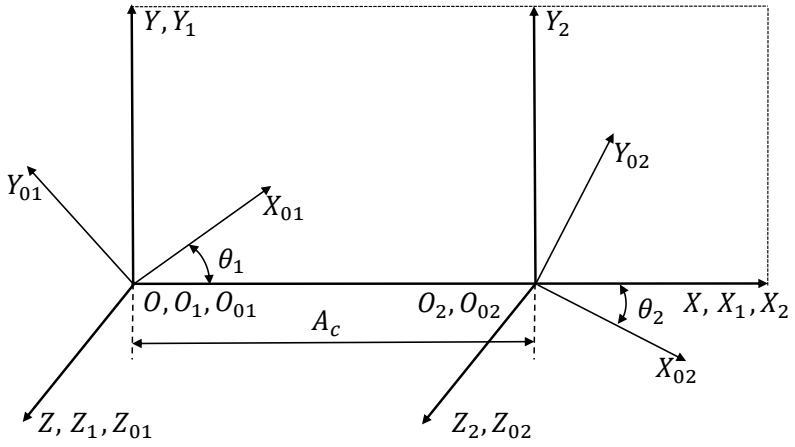

Figure 4 Global coordinate system.

2.1. Global coordinate system

Consider the global coordinate system as $S(X,Y,Z)$ which origin sits in the centre of the main rotor and the Z-axis is along to the rotor axis as shown in Figure 4. The distance between this two coordinate systems is A_c. The main rotor rotate anticlockwise while the gate rotor rotate clockwise. The rotation angles for main and gate rotor are θ_1 and θ_2 separately. The origin and unit vector are defined as shown in the Table 1.

Table 1 Global coordinate system

	Origin	**Unit vector**
Global coordinate system	$\begin{bmatrix} X \\ Y \\ Z \end{bmatrix} = \begin{bmatrix} 0 \\ 0 \\ 0 \end{bmatrix}$	$\begin{bmatrix} \boldsymbol{i} \\ \boldsymbol{j} \\ \boldsymbol{k} \end{bmatrix} = \begin{bmatrix} 1 & 0 & 0 \\ 0 & 1 & 0 \\ 0 & 0 & 1 \end{bmatrix}$

2.2. Rotor coordinate system

In the global coordinate system, the main rotor coordinate is $S_1(X_1, Y_1, Z_1)$ which origin fixes on the centre of the main rotor and Z_1-axis is along the main rotor axis. The gate rotor coordinate is $S_2(X_2, Y_2, Z_2)$ which origin fixes on the centre of the gate rotor and Z_2-axis is along the gate rotor axis. The origins and unit vectors of the rotor coordinate system are defined as shown in the Table 2.

Table 2 Rotor coordinate system

	Origin	**Unit vector**
Main rotor	$\begin{bmatrix} X_1 \\ Y_1 \\ Z_1 \end{bmatrix} = \begin{bmatrix} 0 \\ 0 \\ 0 \end{bmatrix}$	$\begin{bmatrix} \boldsymbol{i_1} \\ \boldsymbol{j_1} \\ \boldsymbol{k_1} \end{bmatrix} = \begin{bmatrix} \boldsymbol{i} \\ \boldsymbol{j} \\ \boldsymbol{k} \end{bmatrix}$
Gate rotor	$\begin{bmatrix} X_2 \\ Y_2 \\ Z_2 \end{bmatrix} = \begin{bmatrix} A_c \\ 0 \\ 0 \end{bmatrix}$	$\begin{bmatrix} \boldsymbol{i_2} \\ \boldsymbol{j_2} \\ \boldsymbol{k_2} \end{bmatrix} = \begin{bmatrix} \boldsymbol{i} \\ \boldsymbol{j} \\ \boldsymbol{k} \end{bmatrix}$

2.3. Rotor transverse local coordinate system

In the main rotor coordinate system $S_1(X_1, Y_1, Z_1)$, the main rotor transverse coordinate system $S_{01}(X_{01}, Y_{01}, Z_{01})$ rotates and transform along the Z_1-axis. In the gate rotor coordinate system $S_2(X_2, Y_2, Z_2)$, the gate rotor transverse coordinate system $S_{02}(X_{02}, Y_{02}, Z_{02})$ rotates and transform alone the Z_2-axis. The origins and unit vectors of the rotor transverse local coordinate system are defined as shown in the Table 3. L is the rotor length. N is the number of cross sections. Ω is the wrap angle.

Table 3 Rotor local transverse coordinate system

	Origin	**Unit vector**
Main rotor	$\begin{bmatrix} X_{01} \\ Y_{01} \\ Z_{01} \end{bmatrix} = \begin{bmatrix} 0 \\ 0 \\ \frac{n_i}{N} \cdot L \end{bmatrix}$	$\begin{bmatrix} \boldsymbol{i_{01}} \\ \boldsymbol{j_{01}} \\ \boldsymbol{k_{01}} \end{bmatrix} = \begin{bmatrix} \cos\left(\frac{n_i}{N} \cdot \Omega_1\right) & -\sin\left(\frac{n_i}{N} \cdot \Omega_1\right) & 0 \\ \sin\left(\frac{n_i}{N} \cdot \Omega_1\right) & \cos\left(\frac{n_i}{N} \cdot \Omega_1\right) & 0 \\ 0 & 0 & 1 \end{bmatrix} \begin{bmatrix} \boldsymbol{i_1} \\ \boldsymbol{j_1} \\ \boldsymbol{k_1} \end{bmatrix}$
Gate rotor	$\begin{bmatrix} X_{02} \\ Y_{02} \\ Z_{02} \end{bmatrix} = \begin{bmatrix} A_c \\ 0 \\ \frac{n_i}{N} \cdot L \end{bmatrix}$	$\begin{bmatrix} \boldsymbol{i_{02}} \\ \boldsymbol{j_{02}} \\ \boldsymbol{k_{02}} \end{bmatrix} = \begin{bmatrix} \cos\left(\frac{n_i}{N} \cdot \Omega_2\right) & \sin\left(\frac{n_i}{N} \cdot \Omega_2\right) & 0 \\ -\sin\left(\frac{n_i}{N} \cdot \Omega_2\right) & \cos\left(\frac{n_i}{N} \cdot \Omega_2\right) & 0 \\ 0 & 0 & 1 \end{bmatrix} \begin{bmatrix} \boldsymbol{i_2} \\ \boldsymbol{j_2} \\ \boldsymbol{k_2} \end{bmatrix}$

2.4. Rotor normal local coordinate system

In addition, the rotor normal coordinate systems are constructed in the rotor coordinate systems. Main rotor normal coordinate system is $S_{11}(X_{11}, Y_{11}, Z_{11})$ as shown in Figure 5(a). The origin O_{11} is along the main rotor pitch helix line and the Z_{11} axis is tangent to the helix line. The $X_{11}Y_{11}$ plane is perpendicular to Z_{11} axis. The main rotor normal profile is defined in the $X_{11}Y_{11}$ plane. Figure 5(b) shows the gate rotor normal local coordinate system.

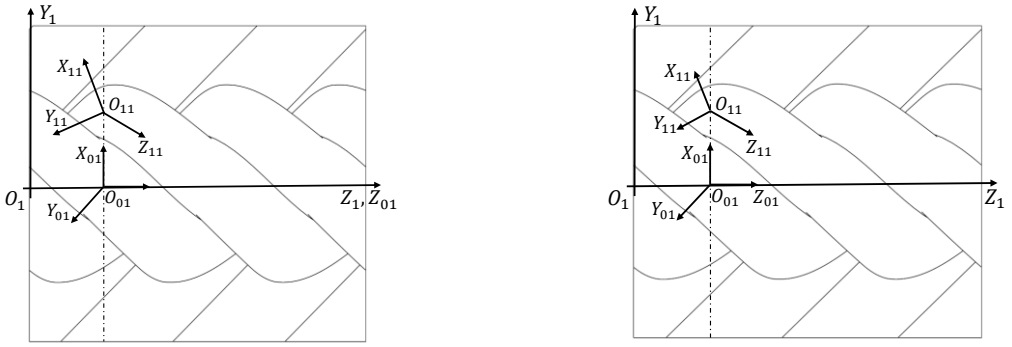

(a) Main rotor (b) Gate rotor

Figure 5 Rotor local *coordinate* system.

The origins and unit vectors of main and gate rotor normal coordinate systems are defined as shown in the Table 4. The origins are along the main rotor pitch helix line. The unit vectors are defined by rotating the unit vector clockwise along the X_{01} axis for helix angle β. The origins and unit vectors have the same definition for the gate rotor normal coordinate system. r_{p1} and r_{p2} are the pitch radius.

Table 4 Rotor local normal coordinate system

	Origin	**Unit vector**
Main rotor	$\begin{bmatrix} X_{11} \\ Y_{11} \\ Z_{11} \end{bmatrix} = \begin{bmatrix} r_{p1} \\ 0 \\ 0 \end{bmatrix}$	$\begin{bmatrix} \boldsymbol{i_{11}} \\ \boldsymbol{j_{11}} \\ \boldsymbol{k_{11}} \end{bmatrix} = \begin{bmatrix} 1 & 0 & 0 \\ 0 & cos(\beta) & -sin(\beta) \\ 0 & sin(\beta) & cos(\beta) \end{bmatrix} \begin{bmatrix} \boldsymbol{i_{01}} \\ \boldsymbol{j_{01}} \\ \boldsymbol{k_{01}} \end{bmatrix}$
Gate rotor	$\begin{bmatrix} X_{12} \\ Y_{12} \\ Z_{12} \end{bmatrix} = \begin{bmatrix} r_{p2} \\ 0 \\ 0 \end{bmatrix}$	$\begin{bmatrix} \boldsymbol{i_{12}} \\ \boldsymbol{j_{12}} \\ \boldsymbol{k_{12}} \end{bmatrix} = \begin{bmatrix} 1 & 0 & 0 \\ 0 & cos(\beta) & sin(\beta) \\ 0 & -sin(\beta) & cos(\beta) \end{bmatrix} \begin{bmatrix} \boldsymbol{i_{02}} \\ \boldsymbol{j_{02}} \\ \boldsymbol{k_{02}} \end{bmatrix}$

2.5. Rack normal coordinate system

The rack is the curve representing a rotor with infinite radius, which meshes with the main rotor profile and gate rotor profile simultaneously. The rack surface is generated by extruding rack curve along helix angle β. Figure 6 shows the normal rack local coordinate system $S_{13}(X_{13}, Y_{13}, Z_{13})$. The Z_{13} axis is along the extruding line and the $X_{13}Y_{13}$ plane is perpendicular to Z_{13}-axis. The right picture shows the rack profile in the main rotor coordinate system.

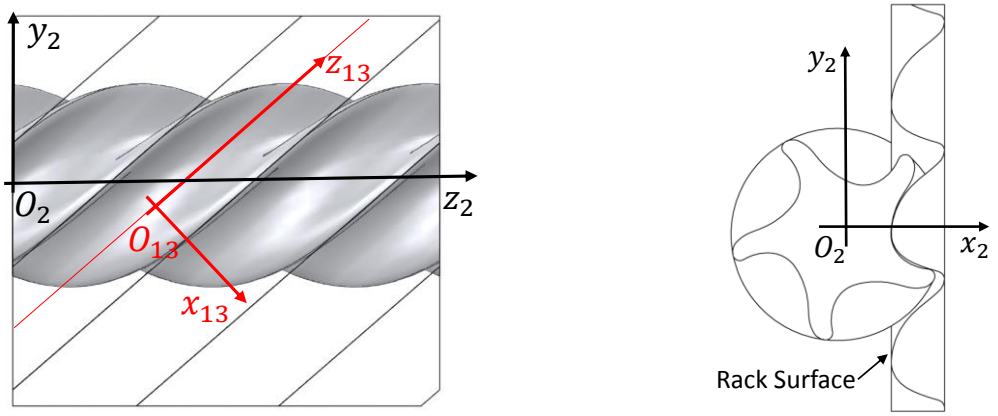

Figure 6 Local coordinate system of main rotor.

The origins and unit vector of the rack normal coordinate system are defined as shown in the Table 5. The origins of rack normal coordinate system are along the rack extruding line. The unit vectors are defined by rotating the main rotor coordinate system unit vector anticlockwise along with the X_{01}-axis.

Table 5 Rack normal coordinate system

	Origin	**Unit vector**
Rack Normal coordinate system	$\begin{bmatrix} X_{13} \\ Y_{13} \\ Z_{13} \end{bmatrix} = \begin{bmatrix} r_{p1} \\ r_{p1} \cdot \frac{n_i}{N} \cdot \Omega_1 \\ \frac{n_i}{N} \cdot L \end{bmatrix}$	$\begin{bmatrix} \boldsymbol{i_{13}} \\ \boldsymbol{j_{13}} \\ \boldsymbol{k_{13}} \end{bmatrix} = \begin{bmatrix} 1 & 0 & 0 \\ 0 & cos(\beta) & sin(\beta) \\ 0 & -sin(\beta) & cos(\beta) \end{bmatrix} \begin{bmatrix} \boldsymbol{i_{01}} \\ \boldsymbol{j_{01}} \\ \boldsymbol{k_{01}} \end{bmatrix}$

3. Decomposition of the fluid domain

The process of replacing a spatial domain by a finite number of discrete volumes constructed with grid points is called gird generation. The spatial domain should be spited to two parts for grid generation. In this case, a 3/5 lobe combination rotors are used.

3.1. Definition of the fluid domain

The fluid domain of a screw rotor is helical type volume generated by the simultaneous revolving of the interlobe space around the rotor axis and translation along the axis. And the fluid domain can be separated to two sub-domain by the rack surface as shown in Figure 7.

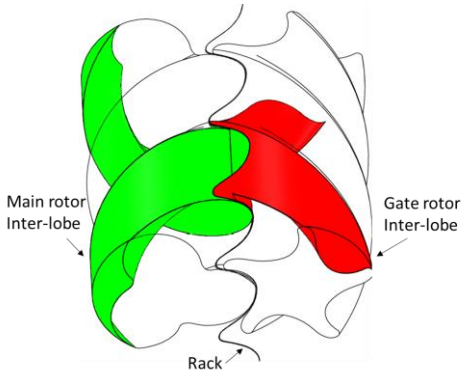

Figure 7 Two sub-domain between the rotors.

3.1.1. The inner boundaries. Firstly the main and gate rotor profiles are input in their own rotor coordinate systems. The profile of the main rotor is one lobe and gate rotor is one interlobe. Because the grid is generated in the interlobe so the lobe of main rotor need to be transformed to the interlobe.

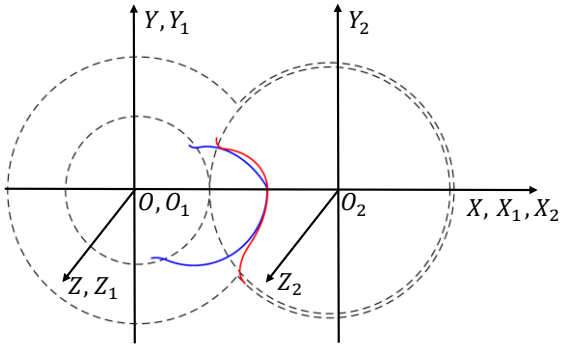

Figure 8 Input Profile.

3.1.2. The outer boundary. The outer boundary is combined the rack and casing. The transverse rack generation method can reference the book writer by Stosic [10] and the normal rack generation method can refer to Wu [11]. The numerical racks are generated for the main and gate rotor separately in the rotor coordinate system as shown in the Figure 9.

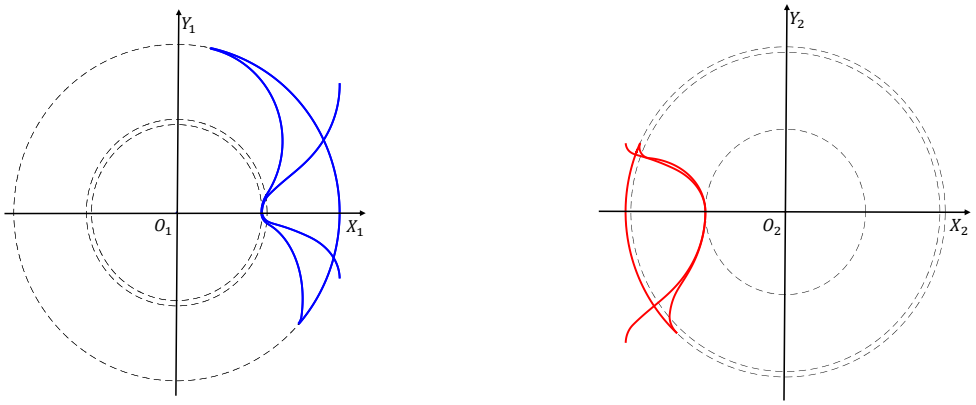

Figure 9. Rotor profile and rack.

3.2. The normal rotor profile and rack.
After getting the rotor profile and rack in the rotor coordinate systems. This inner and outer boundaries can be transformed to different transverse local coordinate systems according to the coordinate system relationship. Then the outer and inner boundaries can be obtained in the normal local coordinate systems.

To demonstrate the changing process of the inner and outer boundaries, Figure 10 shows the sub-domain of the main rotor and gate rotor cut by 21 consecutive normal planes using the method mentioned above. The outer boundary is the composition of the rack and the casing circle and the inner boundary is the rotor profile in the normal plane. With the rotation of the rotors, the normal rack replace part of the casing as the outer boundary gradually cutting in and then out. The grid generation process is implemented in this mathematical boundaries.

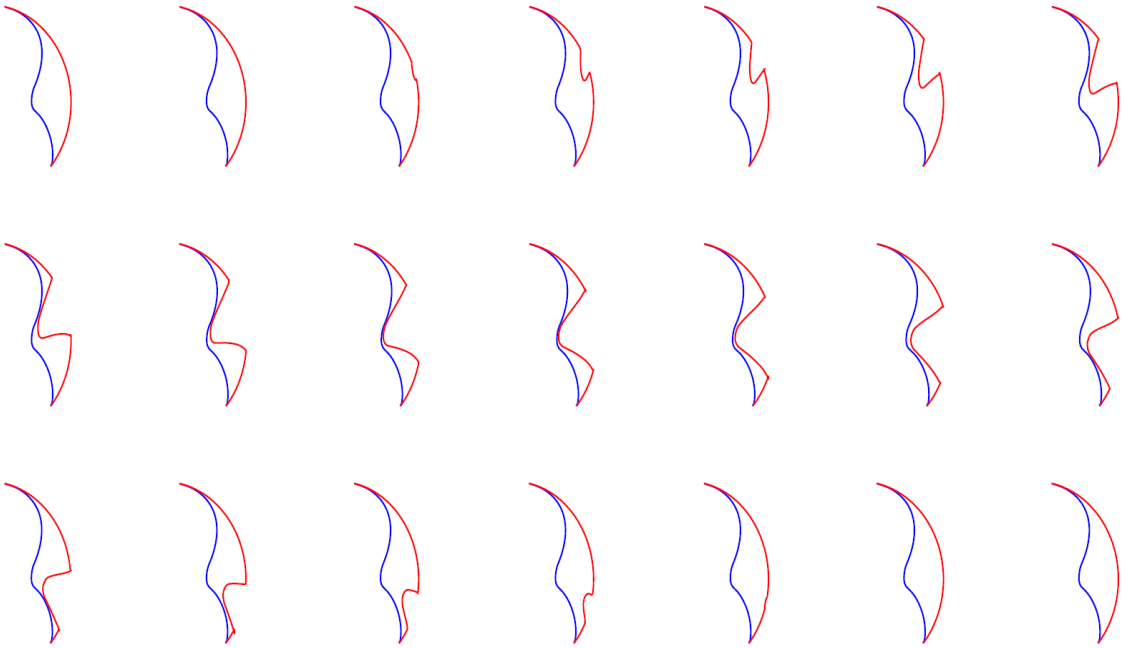

(a) Main rotor (rotor profile is blue line, rack and casing are red line)

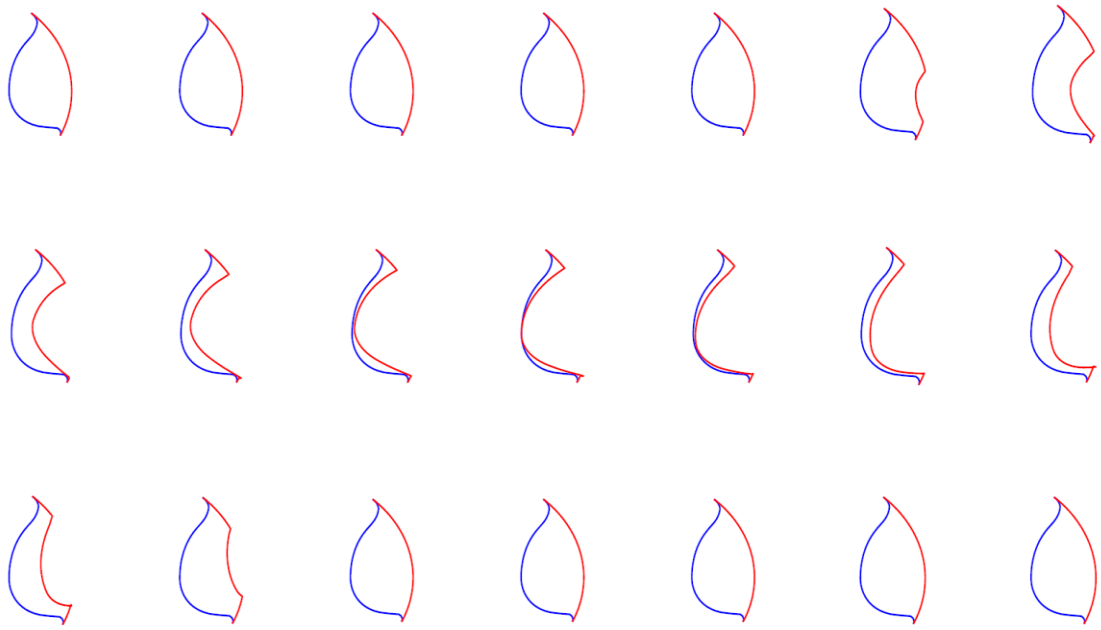

(b) Gate rotor (rotor profile is blue line, rack and casing are red line)
Figure 10 The changing process of the sub-domain

4. Grid generation in normal plane

The customized grid generation tool SCORG is used here as the platform to process the grid generation in the normal cross section. An algebraic grid generation method employing adaptation, transfinite interpolation, grid orthogonalisation and smoothing is used to construct the hexahedral grid in the rotor domain. A subroutine is programmed to generate numerical mesh in the normal plane.

In this case, the rotor configure combination is 3/5. Number of divisions along helix line is 60 and number of divisions along the main rotor sub-domain interlobe ellipse is 60 while along the gate rotor sub-domain interlobe ellipse is 36. Figure 11(1) represents the flow chart of the grid generation subroutine. Figure 11(a), (b) and (c) show the manipulation of the mesh to get hexahedral mesh in the main rotor normal local coordinate system.

4.1. Mapping the outer boundary.

To conduct the structure mesh between the inner and outer boundaries, the number of nodes distributed on the outer boundary should be same as number of nodes on the inner boundary. After the step of rotor profile distribution, the nodes on rotor profile are fixed. They essentially rotate as the rotor turns. But nodes on the casing circles and the rack curve are not fixed. They essentially slide on these curves taking a new position with every rotor turn such that the distribution is always regular. This method is called rotor to casing.

After the inner and outer boundaries of a physical sub-domain have been calculated in the normal plane and the same points distribute on the boundaries by a scanning function which is introduced to interpolate same number of points on the boundaries as shown in Figure 11(a). Then the boundaries have to be mapped to a computational domain. The coordinates of the physical domain are given in $X_{11}Y_{11}$ coordinate system while the computational coordinate are ξ_η. The main rotor sub-domain from tip to tip form an interlobe space which can be mapped from physical region X^n onto a computational domain Ξ^n. Inner boundary of the sub-domain is the rotor profile and the outer boundary is formed by combining the casing circle with the rack curve.

As shown in Figure 11(b), the outer boundary nodes are redistributed according to an arc-length based projection to determine the nodes to be placed on the casing. The redistribution can be controlled by the factor coefficient. The detailed of this redistribution process can be referenced in the book [4].

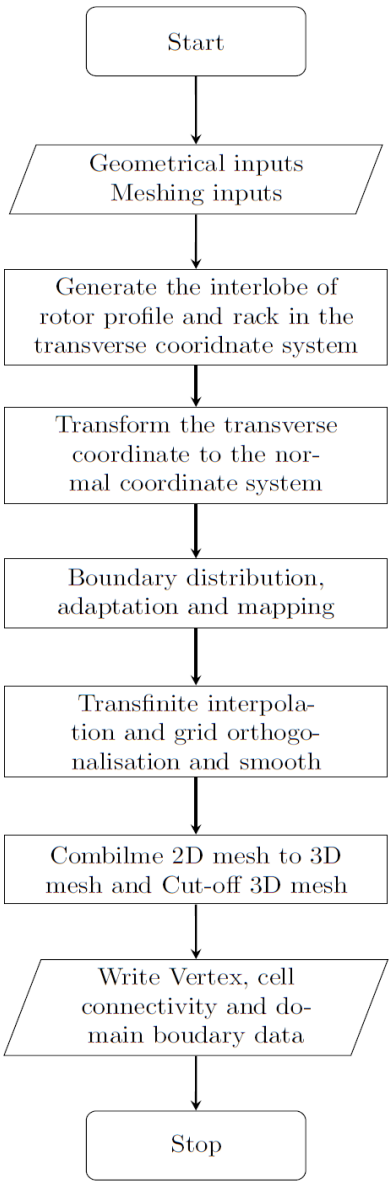

(1) Flow chart of grid generation

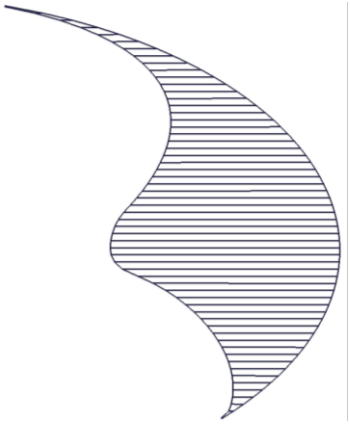

(a) The sub-domain in the normal coordinate system

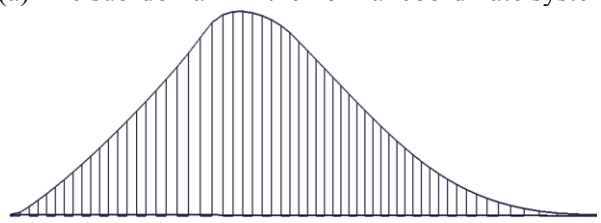

(b) Computational coordinate systems

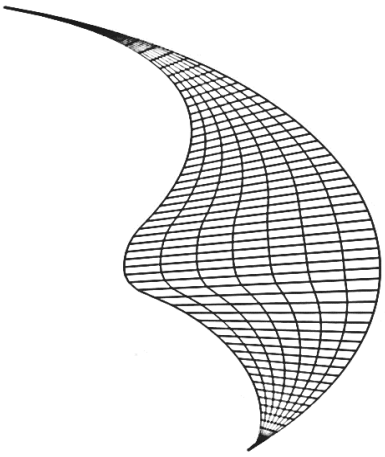

(c) Numerical mesh generated by TFI

Figure 11 Grid generation in the sub-domain

4.2. Transfinite interpolation

Next procedure is to make the inverse transformation from the computational domain to the physical domain according to the new arc-length. The new distribution on the rack is based on previous distribution on the casing by calculation the intersections of the rotor and casing connecting line with the rack.

Once the outer and inner boundaries are distributed same number of nodes, the interior nodes can be distributed in the sub-domain using algebraic transfinite interpolation. The standard transfinite interpolation and a more accurate ortho-transfinite interpolation [12] can be employed here. Figure 11(c) shows the distribution of the interior nodes in the normal plane. The spacing and boundary orthogonality can be controlled. 3-D numerical mesh can be formed by connecting corresponding points in consecutive cross sections. The grid lines will go parallel to the helix line and thus orthogonal mesh will be produced.

Then the Cartesian cut cell method will be implemented for cutting of the flow domain in the end of the rotor. Finally, all the vertexes are exported

5. Conclusions

Algebraic grid generation is widely used for discretization of the working domain for screw machines. In order to align the numerical mesh to the main flow direction and the leakage flow direction, this paper presents the new development of an algebraic grid generation algorithm which uses the normal rack to decompose the fluid domain into two sub-domains. A series of 2D numerical meshes are generated in the planes normal to the rotor pitch helix line. The 2D cross sections are then combined together to construct the full 3D fluid domain representing the main and gate fluid domain. This process makes the grids aligning with the main and leakage flow direction so as to reduce the numerical diffusion and the skewness of the grids in order to increase the stability of the CFD calculation. This method also opens possibility for generating a numerical mesh for single screw machines.

Acknowledgments

This research was supported by China Scholarship Council and the Centre for Compressor Technology at City, University of London.

References

[1] Vierendeels J 2017 Introduction to CFD analysis in positive displacement machines. In: *10th international conference on compressors and their systems,* (London
[2] Kovacevic A 2005 Boundary adaptation in grid generation for CFD analysis of screw compressors *International Journal for Numerical Methods in Engineering* **64** 401-26
[3] Kovačević A 2002 Three-Dimensional Numerical Analysis for Flow Prediction in Positive Displacement Screw Machines. In: *School of Engineering*: City University London)
[4] Kovacevic A, Stosic N and Smith I 2007 *Screw Compressors-Three dimensional computational fluid dynamics and solid fluid interaction* (New York: Springer-Verlag)
[5] Voode J V, Vierendeels J and Dick E 2004 A grid generator for flow calculationsin rotary volumetric compressors. In: *European Congress on Computational Methods in Applied Sciences and Engineering,* (Finland
[6] Rane S and Kovacevic A 2017 Algebraic generation of single domain computational grid for twin screw machines. Part I. Implementation *Advances in Engineering Software* **107** 38-50
[7] Rane S and Kovačević A 2017 Application of numerical grid generation for improved CFD analysis of multiphase screw machines *IOP Conference Series: Materials Science and Engineering* **232**
[8] Rane S, Kovačević A and Stošić N 2015 Analytical Grid Generation for accurate representation of clearances in CFD for Screw Machines *IOP Conference Series: Materials Science and Engineering* **90**
[9] Rane S, Kovacevic A, Stosic N and Kethidi M 2013 CFD grid generation and analysis of screw compressor with variable geometry rotors. In: *8th International Conference on Compressors and their Systems,* pp 601-12
[10] Stosic N, Smith I K and Kovacevic A 2005 *Screw Compressor Geometry Mathematical Modeling and Performance Calculation*: Springer)
[11] Wu Y and Fong Z 2008 Rotor Profile Design for the Twin-Screw Compressor Based on the Normal-Rack Generation Method *Journal of Mechanical Design* **130** 8
[12] Thompson J F, Soni B K and Weatherill N P 1999 *Handbook of Grid Generation*